Virology 448 (2014) 15–25

Contents lists available at ScienceDirect

Virology

journal homepage: www.elsevier.com/locate/yviro

Dengue virus subgenomic RNA induces apoptosis through the Bcl-2-mediated PI3k/Akt signaling pathway

Yi Liu [a,b], Haibin Liu [a], Jing Zou [a,b], Bo Zhang [a], Zhiming Yuan [a,*]

[a] Key Laboratory of Agricultural and Environmental Microbiology, Wuhan Institute of Virology, Chinese Academy of Sciences, Wuhan 430071, China
[b] University of the Chinese Academy of Sciences, Beijing 100039, China

ARTICLE INFO

Article history:
Received 1 July 2013
Returned to author for revisions
22 July 2013
Accepted 18 September 2013
Available online 16 October 2013

Keywords:
DENV-2
Subgenomic RNA
Cytopathicity
Apoptosis
Bcl-2
PI3k/Akt pathway

ABSTRACT

We report a RNA species of 429 nucleotides derived from the 3′ untranslated region of the viral genome in Dengue 2 virus (DENV-2) infected cells. The 3′ terminal of viral RNA contained specific conserved structures that are important for the production of subgenomic RNA. Transient replicon assays suggested that loss of this small RNA has little effect on viral replication, and genetic analysis using recombinant viruses demonstrated that the existence of this subgenomic RNA is not essential for the life cycle of the DENV-2. Results from cytotoxicity and apoptosis assay revealed that the generation of subgenomic RNA is significant for DENV-2 viral cytopathicity and virus-induced apoptosis; and the deficiency could be partially restored by providing subgenomic RNA in trans from transfection. In addition, we found that subgenomic RNA modulates the phosphatidylinositol 3-kinase (PI3k)/Akt signaling pathway through a Bcl-2-related mechanism, resulting in apoptotic cell death.

Introduction

The *Flaviviridae* family comprises three genera: *Flavivirus*, *Pestivirus* and *Hepacivirus*. Most of the flaviviruses are arthropod-borne viruses and mainly transmitted to vertebrate hosts by either mosquitoes or ticks (Gubler et al., 2007). Dengue virus (DENV) belongs to the *Flavivirus* genus and causes potentially fatal diseases in humans and animals. Annually about 50 to 100 million people in the world suffer from dengue fever, including 500 thousand cases of dengue hemorrhagic fever and dengue shock syndrome (Kyle and Harris, 2008). Besides four serotypes of DENV, several members of flaviviruses, such as West Nile virus (WNV), yellow fever virus (YFV), Japanese Encephalitis virus (JEV), and tick-borne encephalitis virus (TBEV), also are major human pathogens (Gould and Solomon, 2008). Currently, no effective antiviral therapy for flavivirus infection is available.

DENV is an enveloped virus with a single-stranded, positive-sense RNA genome about 11 kb in length. The viral RNA consists of one open reading frame (ORF) flanked by highly structured 5′ and 3′ untranslated regions (UTRs) (Gubler et al., 2007). The single open reading frame encodes ten viral proteins required for the viral life cycle, including three structural proteins [capsid (C)-premembrane (prM)-envelope (E)] and seven non-structural proteins (in the order NS1-NS2A-NS2B-NS3-NS4A-NS4B-NS5) (Lindenbach et al., 2007; Rice et al., 1985). The structural proteins form viral particles and mediate virus entry, while the nonstructural proteins participate in viral replication, virion assembly (Kummerer and Rice, 2002; Liu et al., 2003) and invasion of innate immune response (Guo et al., 2005; Munoz-Jordan et al., 2003). The conserved nucleotide sequence and secondary structure in the UTRs of DENV serve various functions in viral translation, RNA replication, and encapsidation (Markoff, 2003). The DENV 5′ UTR contains two RNA secondary structures, a large stem-loop (SLA) and a short stem-loop (SLB) (Gebhard et al., 2011). The SLA and SLB structures have been shown to be necessary for viral RNA synthesis (Alvarez et al., 2005; Filomatori et al., 2006; Yu et al., 2008). Specific structures at the 3′ end of the viral genome also serve crucial roles in replication, especially the terminal stem-loop structure (3′ SL) (Zeng et al., 1998). The importance of 3′ SL for DENV and other flaviviruses is supported by a variety of experimental evidence (Brinton et al., 1986; Hahn et al., 1987; Yu and Markoff, 2005; Zeng et al., 1998).

Apart from the genome RNA (gRNA), a mass of subgenomic RNA (sgRNA) derived from the 3′ UTR is found in infected cells with Murray Valley encephalitis (MVE), JEV, WNV, and DENV (Liu et al., 2010). The small noncoding RNA is a unique characteristic of the *Flavivirus* genus, and possibly has a significant effect on virus–host interaction in the viral life cycle. In WNV and YFV it has been demonstrated that the accumulation of sgRNA is a product of incomplete degradation of viral genome RNA by exoribonuclease

* Corresponding author. Fax: +86 27 87198120.
E-mail address: yzm@wh.iov.cn (Z. Yuan).

0042-6822/$ - see front matter © 2013 Elsevier Inc. All rights reserved.
http://dx.doi.org/10.1016/j.virol.2013.09.016

XRN1. Additionally, sgRNA in WNV is essential for viral cytopathicity in cells and pathogenicity in mice (Pijlman et al., 2008; Silva et al., 2010). Some secondary structures and RNA pseudoknot interactions in 3′ UTR are required for flaviviral sgRNA generation (Funk et al., 2010; Yang et al., 2002). Furthermore it has been proved that sgRNA contributes to WNV evasion of the type I interferon-mediated antiviral response (Schuessler et al., 2012) and other research reveals sgRNA may modulate JEV translation and replication (Fan et al., 2011). More recently, a study has demonstrated that sgRNA displays as a nucleic acid-based regulator of RNAi pathways in WNV (Schnettler et al., 2012). However, the mechanism of this small sgRNA production and its function in DENV lifecycle remains unknown.

Apoptosis has been observed as a result of flavivirus infection (Despres et al., 1996) since host cells are thought to activate biochemically distinct apoptotic pathways when they encounter a flavivirus. In the JEV-induced apoptosis endoplasmic reticulum (ER) stress might participate, triggering p38 MAPK activation and CHOP induction (Su et al., 2002). Thus, cells infected with WNV can cause caspase-3 and -9 activations through the mitochondrial pathway (Chu and Ng, 2003). Growing evidence shows that Dengue virus infection will trigger apoptotic cell death in vitro and in vivo in a cell-dependent manner. Although many intracellular signaling systems are involved in the induction of apoptosis in Dengue virus infected cells, the underlying molecular processes are not well characterized (Courageot et al., 2003).

In this paper, we report a RNA species present in DENV-2-infected cells. Northern blot showed that kinetics of sgRNA appearance paralleled that of DENV-2 genome. Using primer extension we determined the sgRNA was 429 nt in length and corresponded to the 3′ terminus of the genome. Mutagenesis studies proved that some conserved motifs in region II of 3′ UTR were crucial for sgRNA generation. Combining the results from DENV-2 replicons and infectious cDNA clones, we concluded that sgRNA had little effect on viral life cycle, but demonstrated sgRNA production was necessary for viral cytopathicity in cell culture. Furthermore we elucidated a novel role for sgRNA as a determinant in DENV-2 virus-induced apoptosis pathway. The data is important for further study of the DENV life cycle and virus–host interaction, as well as for the therapeutical treatment of DENV infection.

Results

Identification of subgenomic RNA in DENV-2

Northern hybridization with the corresponding 3′ UTR-specific probe showed that Vero cells infected with DENV-2 (TSV01 strain) produced a subgenomic RNA (sgRNA) of about 400 nucleotides (nt) in size (Fig. 1A—Lane VERO). Total RNA was extracted from the mammalian cells at 48 h post infection (p.i.), and were analyzed using a DIG-labeled oligonucleotide, complementary to nt 10,622 to nt 10,723 in the DENV-2 3′ UTR as a probe. In addition, experiment with viral RNA extracted from DENV-2 showed that sgRNA was not packaged into mature dengue virions (Fig. 1A—Lane DEN-2). On the basis of sgRNA estimated length, we assumed its 5′ initiation would be located in the viral 3′ UTR. Primer extension of a 5′-biotinylated oligonucleotide, complementary to DENV-2 nt 10,360 to nt 10,384 and sequence analysis revealed that the 5′ end of the DENV-2 sgRNA was residue A at position 10,295 (Fig. 1C). Combined with the genome size of DENV-2 we determined the length of DENV-2 sgRNA was 429 nt. In order to elucidate the mechanism of sgRNA generation, we examined whether the structural proteins or viral replication were involved. We electroporated BHK-21 cells with DENV-2 nonreplicating replicon RNA and DENV-2 wild type replicon RNA, at the same time we transfected pSUPER-3′ UTR vector with liposome and extracted the total RNAs. In experiments with dengue replicon RNA and pSUPER-3′ UTR vector, we clearly found that sgRNA could be easily detected in cells transfected with all constructs (Fig. 1B), replicating (DEN-2 Rep) or nonreplicating (Rep-NS5 Mut), thus clarifying that viral proteins and RNA replication were dispensable for sgRNA production. The replication defective RNA was designed by replacing the essential GDD motif of the RNA dependent RNA polymerase NS5 by AAA (DVRep-NS5Mut) (Khromykh et al., 1998).

Time course study of sgRNA and viral genome yield in DENV-2 infected cells

To determine the kinetics of appearance of the sgRNA and genomic RNA (gRNA), BHK-21 and Vero cells were infected with DENV-2 at a multiplicity of infection (MOI) of 0.5. Then total RNAs were isolated at the indicated times post-infection and analyzed by Northern Blot. The result showed that both gRNA and sgRNA can be detected up to 48 h post infection in two cell types. Throughout the experiment, the abundance of sgRNA continued to increase and was obviously much greater than that of gRNA (according to the size and densities of the bands) (Fig. 2A and B).

RNA structure/sequence requirements for sgRNA generation

The 451 nt long DENV-2 (TSV01 strain) 3′ UTR can be divided into three regions (Fig. 3A). These harbored a number of specific structures which played important roles, including structure X at the 5′ end, conserved (repeated) sequences (CS2 and RCS2), top loop of hairpins (TL1/2), a cyclization sequence and a conserved stem-loop structure at the 3′ end (3′ LSH) (Ramanathan et al., 2006). To investigate the RNA structures responsible for sgRNA generation, we constructed a series of deletion mutations in the 3′ UTR (Fig. 3B) and tested their effect on sgRNA production in infected cells (Fig. 3C). Northern blot analysis indicated that deletions in AU-rich region (M1), structure X (M2), TL1 (M3), RCS2 (M4), TL2 (M5), CS2 (M6), and region I (M7) did not affect sgRNA production, and M3 and M4 viruses produced less abundance of sgRNA than the others. Most importantly, only the deletion in region II (M8) led to the total loss of sgRNA.

SgRNA production is not required for the life cycle of DENV-2

For studying the effect of the full length and amount of sgRNA on viral life, BHK-21 cells were transfected with equal amounts of replicon RNAs of the wild type (WT) and the mutants, and the luciferase activities at various time post transfection were recorded. By using a DENV-2 transient replicon assay, RNA translation and amplification could be assayed through the expression of luciferase at 6 h and 60 h after transfection. As shown in the figure (Fig. 4A–C), all mutations did not affect the translation of input RNA. Except for DVRep-NS5Mut, which was a replication defective mutation, other mutant replicons maintained almost the same level of luciferase signals as the wild type after 24 h post transfection. We then assessed their corresponding E protein expression and growth in mammalian cells. At 96 h post infection wild type and recombinant viruses all expressed E protein normally using IFA (Fig. 4D). Growth kinetics among wild type and the mutants exhibited slight differences (Fig. 4E). Mutations including M1, M2, M5–M7 almost kept pace with WT in viral lifecycle, while viral titers in M3 and M4 were lower than that of WT. Mutation M8 showed a slight delay in initial virus production compared to the WT, so its lifecycle lagged a little. Collectively, mutations (including M1–M8) did not have a major effect on viral translation, replication, E protein expression or viral lifecycle. But generation of abundant full-length sgRNA made the virus more effective.

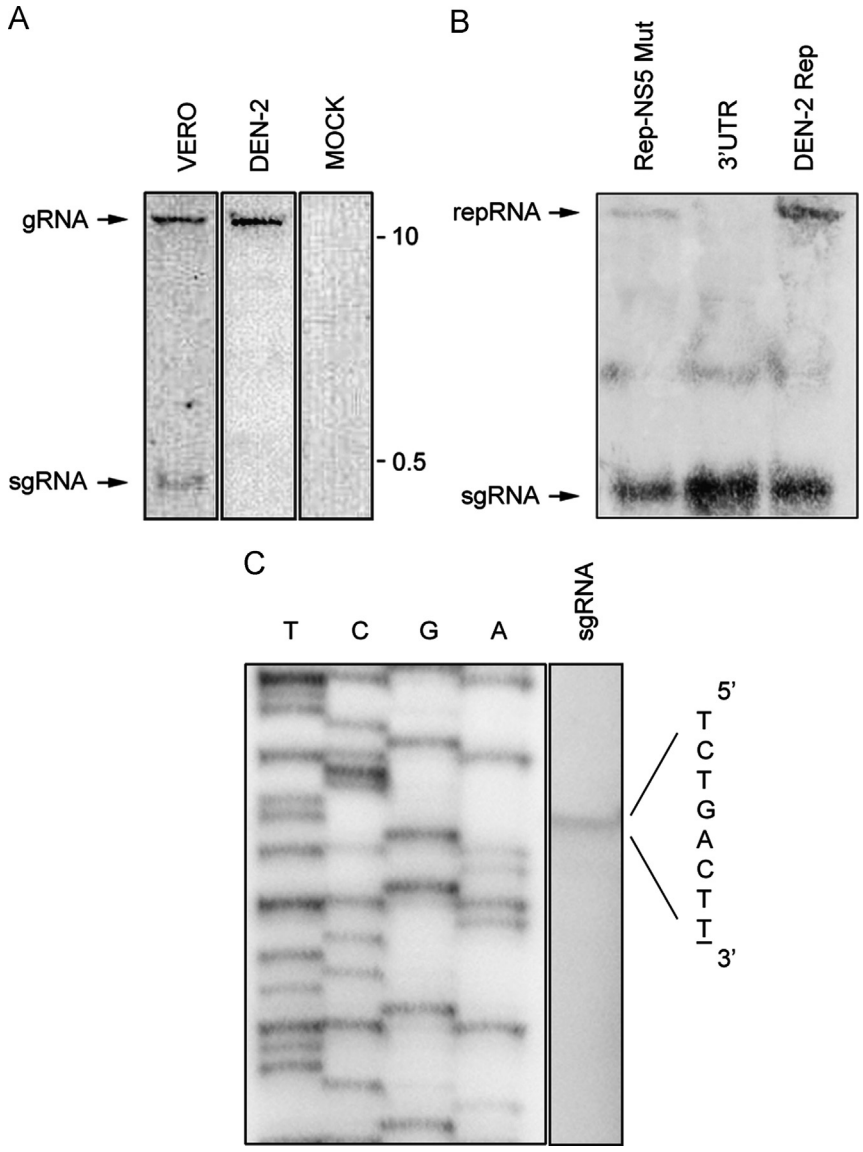

Fig. 1. Accumulation of subgenomic RNA in DENV-2-infected cells. (A) Subgenomic RNA production in Vero cells. The mammalian cell line Vero was infected with DENV-2 at a multiplicity of infection (MOI) of 1. At 72 h p.i., total RNAs were isolated and analyzed by Northern blotting. Lane Vero, DENV-2 infected Vero cells. Lane DENV-2, DENV-2 mature virions. Lane MOCK, uninfected Vero cells. Size markers are indicated on the right. Bands corresponding to the DENV-2 genome and subgenomic RNA are indicated by arrows. (B) Northern blot of RNAs isolated from BHK-21 cells electroporated with DENV-2 nonreplicating replicon RNA containing the GDD motif of the RNA dependent RNA polymerase NS5 by AAA, pSUPER-3′ UTR vector, or DENV-2 wild type replicon RNA. Bands corresponding to the DENV-2 replicon genome and subgenomic RNA are indicated by arrows. (C) Primer extension analysis using 5′-biotinylated oligonucleotide, which is complementary to DENV-2 nt 10,360 to nt 10,384. pACYC TSV replicon was sequenced with the same oligonucleotide to obtain a sequencing ladder for determination of the 5′ end of the subgenomic RNA. At least three independent experiments were performed.

SgRNA production is of significant importance for viral cytopathicity in cell culture

In order to illuminate the function of sgRNA, we first compared plaque morphology between wild type and recombinant viruses by SIA (Fig. 5A). The results indicated that for the following mutations abolishing sgRNA production (M8) showed no visible plaque formation, and lower abundance of sgRNA production mutants (M3 and M4) showed vague plaque formation. The rest of the mutations and the wild type formed clear and visible plaques. In addition we performed plaque assay by immunostaining for better observation (Fig. 5B). To confirm the obvious discrepancy in plaque formation, a quantification experiment by released crystal violet stain revealed that most mutants and the wild type caused death of about 70% of cells at 8 or 9 days p.i., while M3 and M4 gave about 40% and M8 only 10% or less (Fig. 5C). This difference in viral cytopathic effect was also validated in MTT assay by measuring SDH release from cells into the culture supernatant (Fig. 5D).

sgRNA production is indispensable in DENV-2-induced apoptosis pathway

Since there was significant contrast of cytopathic effect during virus infection, we further evaluated the apoptosis rate of infected cells at 4 days p.i. at an MOI of 1. In the flow cytometry assay, approximately 50% of BHK-21 cells underwent apoptosis in the wild type and other mutants with the exception of M8 (Fig. 6A). The mutant M8 could not induce apoptosis in the infected BHK-21 cells at various multiplicities of infection (data not shown). To explore the possible mechanism responsible for the DENV-2

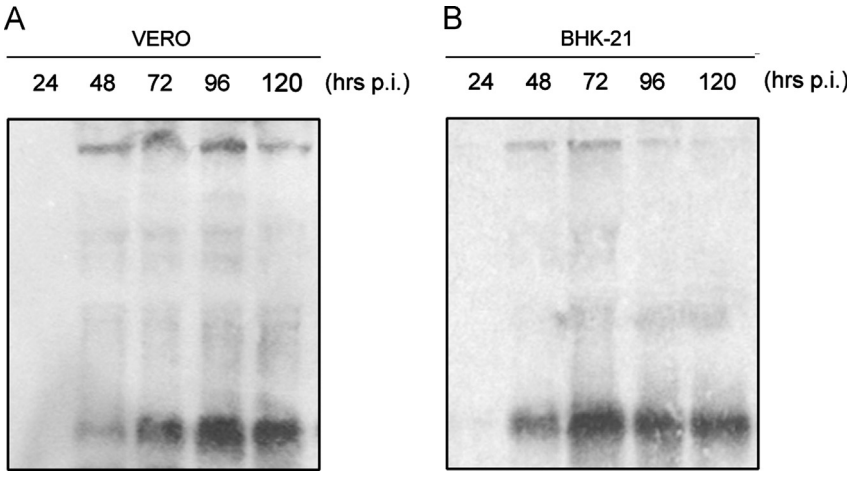

Fig. 2. Kinetics of genomic and subgenomic RNA synthesis in DENV-2-infected mammalian cells. (A) Northern analysis of total RNAs isolated from DENV-2-infected Vero cells at indicated time points post infection. Cells were infected with DENV-2 at an MOI of 0.5. (B) Total RNAs from DENV-2-infected BHK-21 cells were analyzed by Northern blotting using DIG-labeled oligonucleotide, complementary to nt 10,622 to nt 10,723 in the DENV-2 3′ UTR as a probe. Cells were infected with DENV-2 at an MOI of 0.5. At least three independent experiments were performed.

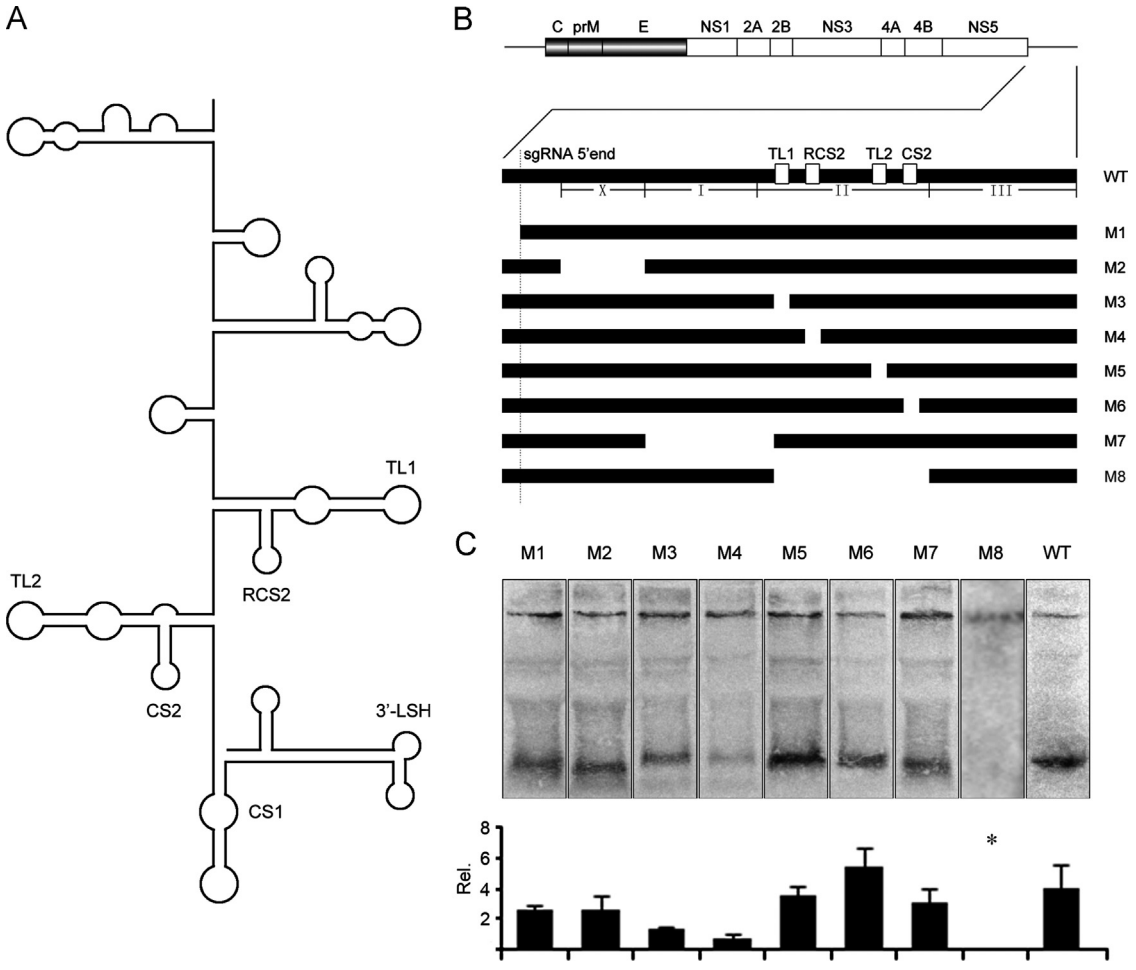

Fig. 3. Structure/sequence required for the production of subgenomic RNA. (A) RNA structure model of DENV-2 3′ UTR generated from previously described (Proutski et al., 1997). TL1/2, top loop of hairpins; (R) CS1/2, (repeated) conserved sequence; 3′-LSH, 3′ long stable hairpin structure. (B) Schematic representation of the DENV-2 genome organization, 3′ UTR and introduced deletions. Subgenomic RNA 5′ end at position-429 is indicated. (C) Northern blot of RNAs isolated from BHK-21 cells infected with recombinant viruses. The relative intensities of the subgenomic RNA bands were calculated by using the band intensity of wild type genome RNA for each group as the denominator and are indicated for each lane. The asterisks indicate that the differences are statistically significant (*, $P < 0.05$; **, $P < 0.001$). The data shown represented the mean values and standard deviations of the results. Three independent experiments, repeated three times for each sample, were performed.

induced apoptotic pathway, we analyzed caspase-3 and Poly ADP-ribose polymerase (PARP) cleavage by Western blotting. Caspase-3 is one of the key executors of apoptosis, and its activation leads to downstream cleavage of PARP. Using the antibody to recognize the endogenous levels of full-length caspase-3 (35 kD) and the large fragment of caspase-3 (17 kD) resulting from cleavage we found

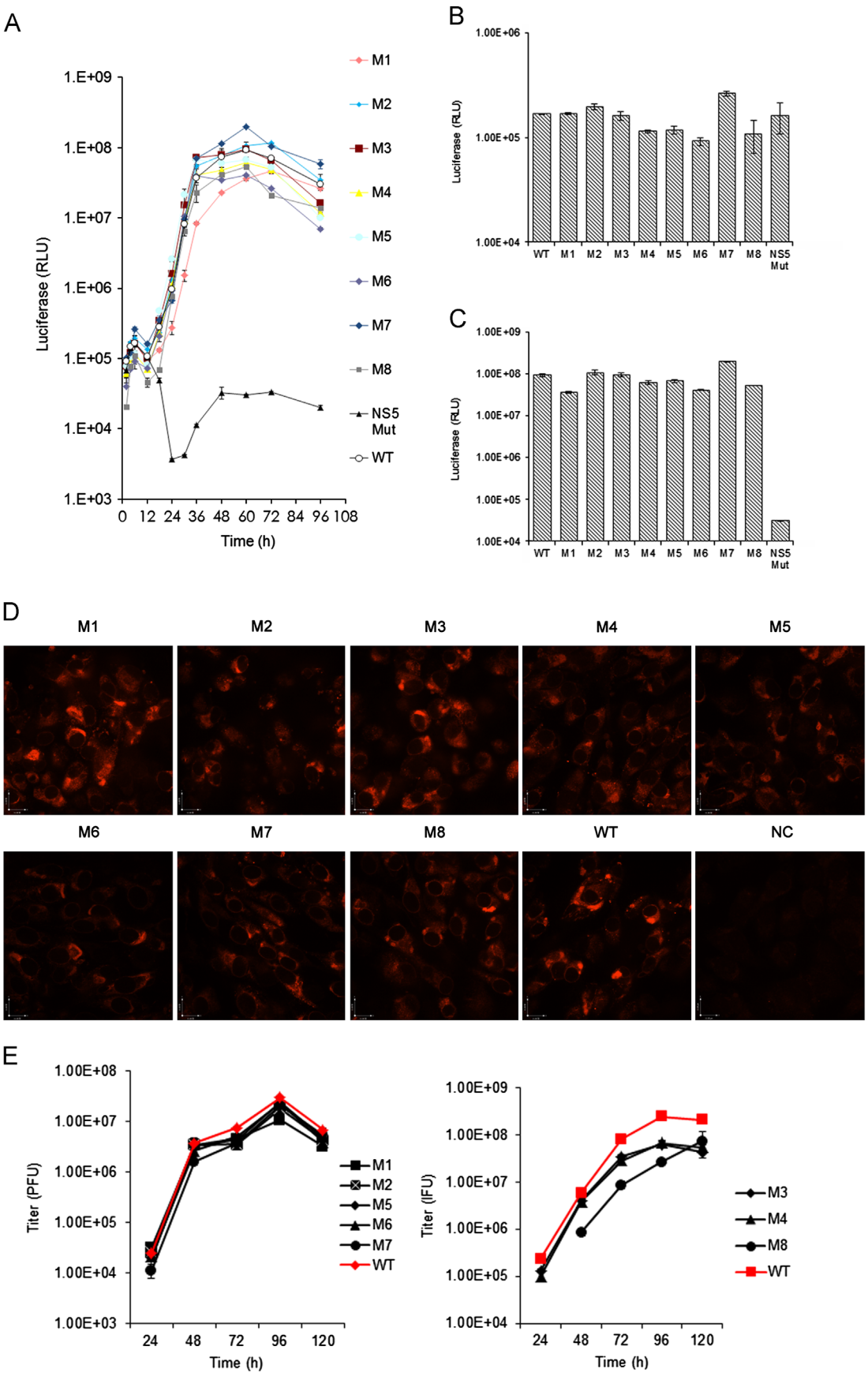

Fig. 4. Subgenomic RNA is not essential for DENV-2 life cycle. (A) BHK-21 cells were electroporated with equal amounts (10 μg) of WT, M1–M7, or M8 mutant replicon RNAs. The transfected cells were harvested at the indicated time points post transfection and *Renilla* luciferase activities (RLU) were measured. Each data point is a log10 value of the average of luciferase signals from three independent experiments; the error bars indicate standard deviations. (B) and (C) Luciferase activities were measured separately at 6 h and 60 h post transfection (BHK-21 cells). The data represented here were obtained from 4A. (D) BHK-21 cells were infected with equal MOI of WT or M1 to M8 mutant viruses. The infected cells were monitored for viral E protein expression by immunofluorescence assay at 96 h p.i. Anti-E monoclonal antibody 4G2 and Texas Red goat anti-mouse IgG were used as primary and secondary antibodies, respectively. Representative microscope images were presented. (E) Viral growth kinetics of DENV-2 wild type and the M1 to M8 mutants in BHK-21 cells. BHK-21 cells were infected at an MOI of 1, and the medium of infected cells was sampled at indicated times post infection. Titers were determined by plaque assays on BHK-21 cells with 1% crystal violet stained for M1, M2, M5–M7 and with immunoperoxidase staining for M3, M4 and M8. The data represented three independent experiments performed in duplicate.

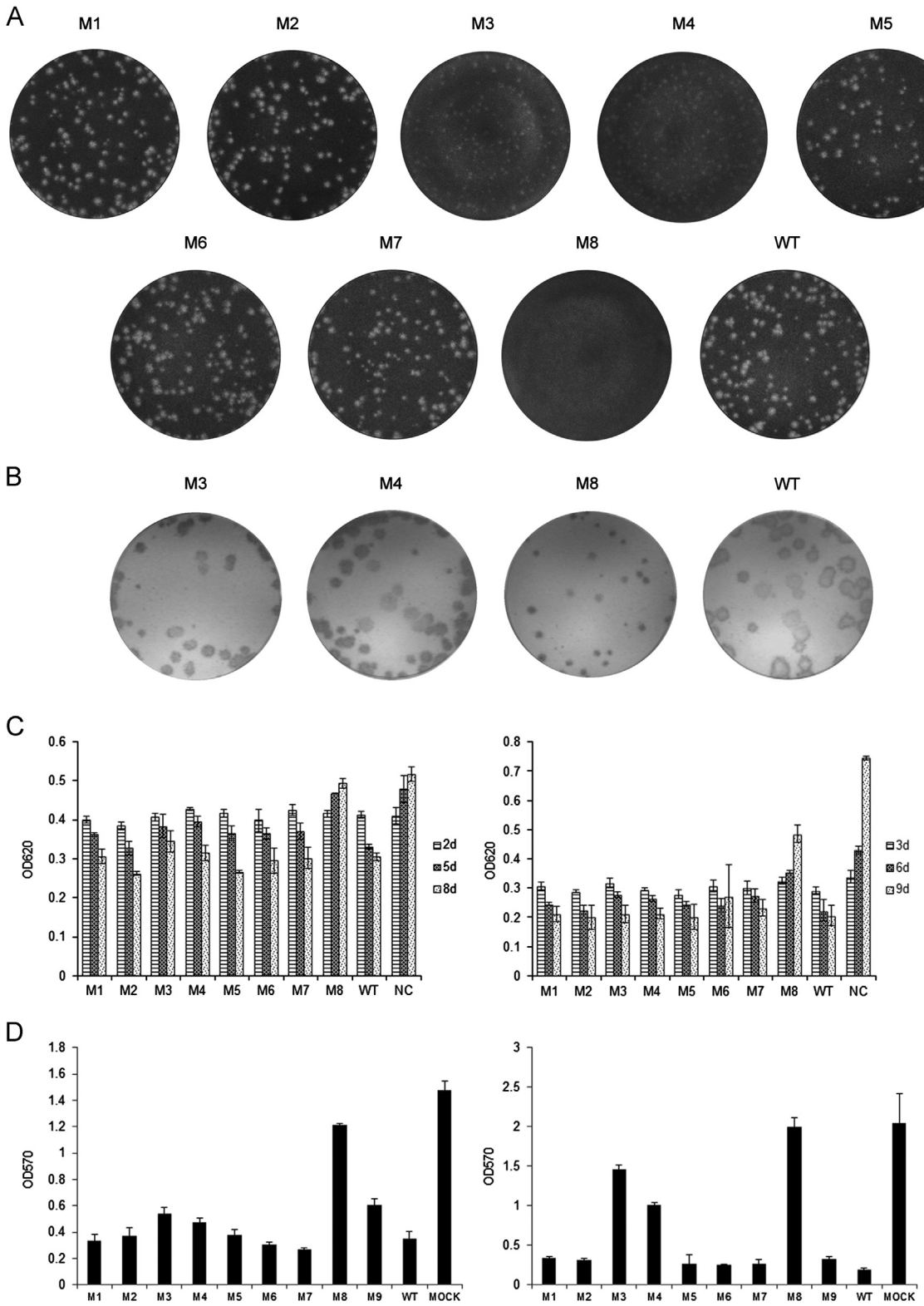

Fig. 5. Subgenomic RNA is required for viral cytopathicity in cell culture. (A) Plaque morphology of DENV-2 wild type and recombinant viruses by specific infectivity assay. (B) Plaque morphology of DENV-2 wild type and M3, M4, M8 recombinant viruses using immunoperoxidase staining. (C) Vero and BHK-21 cells were infected at an MOI of 0.1 with DENV-2 wild type and mutant M1 to M8 viruses and fixed at indicated time points after infection. Crystal violet was released from cells by methanol and OD 620 nm was measured. Average results and standard deviations from three independent experiments were presented. The left, Vero cells; the right, BHK-21 cells. NC, negative control. (D) MTT assays. SDH release into cell culture fluid of Vero and BHK-21 cells was measured. Cells were infected with DENV-2 wild type and mutant M1 to M8 viruses at an MOI of 0.1. Average results and standard deviations from three independent experiments were presented. The left, Vero cells; the right, BHK-21 cells. Mock, negative control.

that mutants M1–M7 and WT could cause caspase-3 cleavage but not mutant M8 (Fig. 6B). Also, caspase-3 activation finally resulted in cleavage of PARP [full-length PARP (116 kD) and the C-terminal catalytic domain (89 kD)] (Fig. 6C). These data suggested that sgRNA may play an important role in the DENV-2 induced apoptotic pathway in a caspase-3-dependent manner.

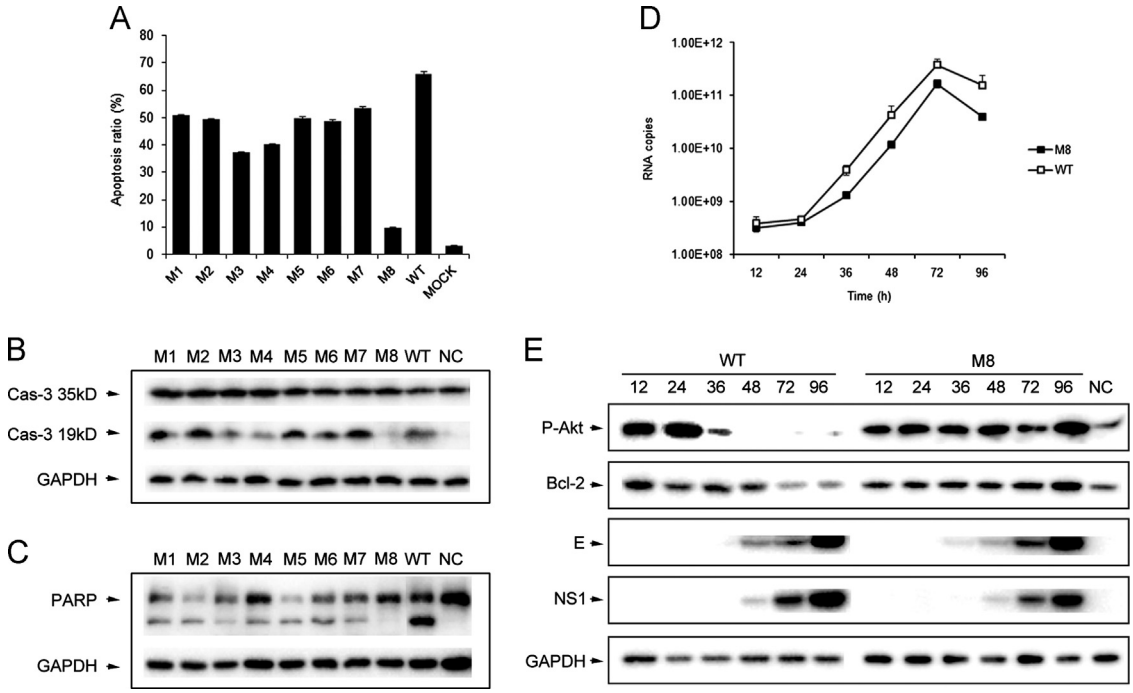

Fig. 6. Subgenomic RNA requirement for apoptosis pathway. (A) Apoptosis assays. BHK-21 cells were infected with DENV-2 wild type and mutant M1 to M8 viruses at an MOI of 1. After 96 h post infection, the cells were collected and analyzed by flow cytometry using Annexin V-FITC/PI staining. Representative data of three independent experiments are shown here. (B) and (C) Caspase-3 (B) and PARP (C) cleavage in infected cells. BHK-21 cells were infected with DENV-2 wild type and mutant M1 to M8 viruses at an MOI of 1 and were lysed at 96 h p.i. Western blotting was performed with the antibodies for caspase-3 (B), PARP (C), and GAPDH. NC, negative control. At least three independent experiments were performed. (D) Kinetics of the M8 mutant and wild type genome RNA synthesis in infected BHK-21 cells. The cells were infected at an MOI of 1, and extracted RNA were subjected to real-time RT-PCR assay. Average results and standard deviations from three independent experiments were presented. (E) Kinetics of protein Akt phosphorylation, Bcl-2, envelope E and NS1 expression level in DENV-2 wild type and M8 mutant. BHK-21 cells were infected at an MOI of 1 and then the cells were cultured for various periods (in hours) as indicated at the top. The cell lysates were harvested for Western blot analysis with the specific antibodies for Ser473-phospho-Akt, Bcl-2, E, NS1 and GAPDH. NC, negative control. At least three independent experiments were performed.

To better understand different apoptotic signaling pathways between M8 and WT, we examined this in more detail. To compare the viral replication level, we extracted total cellular RNAs from the M8 and WT infected cells; the viral RNA amounts were quantified using one-step real-time RT-PCR. Meanwhile, structural protein E and nonstructural protein NS1 were also quantified using Western blotting throughout the experimental period. The standard curve obtained from known input copies was determined (data not shown). From Fig. 6D, the genomic RNA of M8 mutant in infected BHK-21 cells was as much as that of WT for the first 24 h p.i. In the remaining experimental time, the accumulation of the M8 genome followed the same trend as the wild type genome but statistical analysis showed that at 36 h p.i. the amount was less by three to four times. The expression levels of protein E and NS1 in both M8 and wild type infected cells were approximately equal (Fig. 6E).

To define the pathway by which sgRNA leads to apoptosis, we examined the activation of phosphatidylinositol 3-kinase/Akt signaling in the DENV-2-infected BHK-21 cells. The phosphorylation status of Akt was monitored by Western blot using an antibody specific to phosphor-Akt (ser473). Cells infected with wild type and M8 at an MOI of 1 were lysed at various time points post infection. The amounts of phosphorylated Akt were plentiful in wild type and M8 infected cells around 12 h to 24 h post infection (Fig. 6E). At the later stages the protein levels of phosphorylated Akt in the wild type were found to be reduced gradually but not in the M8 mutant. These results suggested that both the wild type and M8 could activate Akt phosphorylation after virus infection and that Akt phosphorylation level was maintained for longer in M8-infected cells than in the wild type.

Subsequently, we used an antibody specific to the bcl-2 protein and we found the expression level of bcl-2 between the WT and mutant M8 was different. Cells infected with WT and M8 at an MOI of 1 were lysed at indicated times post infection. As shown in Fig. 6E, the bcl-2 protein was evident in the wild type starting from 12 h to 36 h p.i. but later its amount began to decrease to a much lower level. In contrast, the bcl-2 protein in M8-infected cells maintained a high expression level throughout infection.

Complementation experiment with sgRNA

To confirm the role of sgRNA in virus-induced cytopathicity and apoptosis, the defect in sgRNA production was complemented by providing sgRNA in trans from transfected vector pSUPER-sgRNA. The cytopathicity and apoptosis of M8 were partially restored in sgRNA-existing cells. In cells producing sgRNA the M8 mutant can form visible plaques (Fig. 7A), and also the cytopathic effect with released crystal violet stain (Fig. 7B) and the apoptotic rate were significantly increased (Fig. 7C). Due to a transfection efficiency of about 50%, the compensation was limited. In addition, sgRNA alone could not induce cell death or even apoptosis, indicating that sgRNA must act under the condition of viral infection to promote virus-induced cytopathicity and apoptosis.

Discussion

Recent work has demonstrated that members of the *Flavivirus* genus can produce abundant, subgenomic, noncoding RNA derived from the 3′ untranslated region of genome RNA (Pijlman et al., 2008). In this study, we have identified cells infected with DENV-2 (TSV01 strain) that generate a RNA species. This subgenomic noncoding RNA is of viral origin and not packaged into mature virions. Viral proteins, RNA replication or even 5′ UTR is not

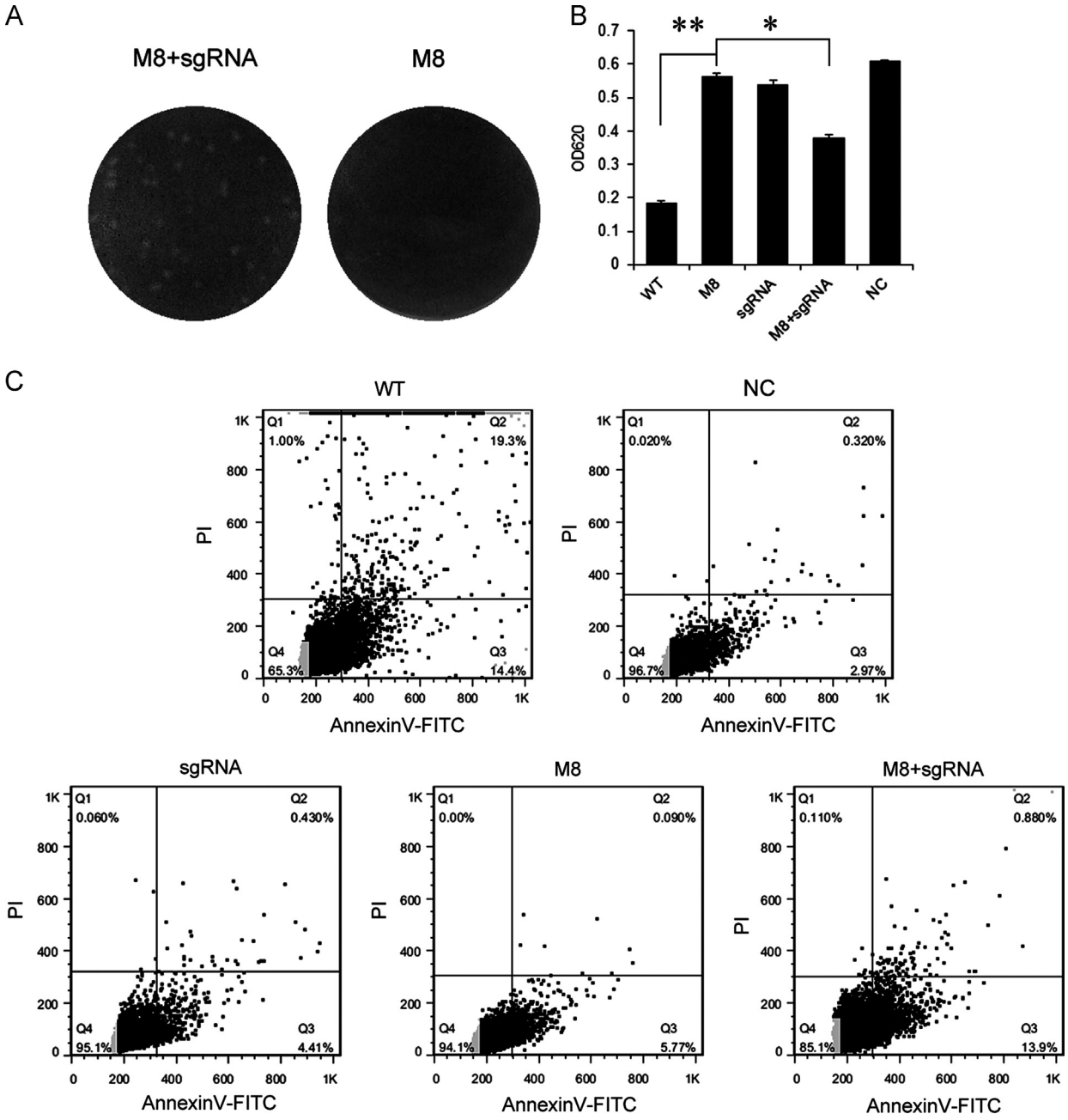

Fig. 7. Partial rescue of virus-induced cytopathicity and apoptosis by complementation with subgenomic RNA. (A) Viral plaque formation by sgRNA complementation. BHK-21 cells were transfected with pSUPER-sgRNA. After 24 h cells were infected with recombinant M8 virus, overlaid and stained at 5 days p.i. (B) Partial rescue of virus-induced cytopathicity. BHK-21 cells were transfected with subgenomic RNA-producing plasmid pSUPER-sgRNA. At 24 h post transfection, cells were infected with mutant M8 at an MOI of 0.1. Cells infected with wild type or untreated were used as controls. At 8 days post infection, crystal violet released from cells by methanol was measured at OD 620 nm. NC, negative control. The asterisks indicate that the differences are statistically significant (*, $P < 0.05$; **, $P < 0.001$). The data shown represented the mean values and standard deviations of the results. Three independent experiments, repeated three times for each sample, were performed. (C) Partial rescue of virus-induced apoptosis. BHK-21 cells were transfected with subgenomic RNA-producing plasmid pSUPER-sgRNA. At 24 h post transfection, cells were infected with mutant M8 at an MOI of 1. Cells infected with wild type or untreated were used as controls. Apoptosis assays were performed at 96 h p.i. NC, negative control. Representative data of three independent experiments were shown here.

responsible for its production (Fig. 1). Thereby, some cellular proteins or factors are possibly involved in sgRNA biogenesis. A previous study indicated that the host exoribonuclease XRN1 hydrolyzed the viral genome in a 5′–3′ direction yielding sgRNA (Silva et al., 2010). In our study, genetic analysis using DENV-2 full-length infectious clones and recombinant viruses revealed that conserved structures in the viral 3′ UTR are crucial for the production of full-length sgRNA. Combined with Northern blot, each deletion in structure X, region I, TL1, RCS2, TL2 or CS2 did not cause the loss of sgRNA except for deletions in region II (Fig. 3). Thus we conclude that the sequence in region II in 3′ UTR may act as a signal to XRN1. Since the separate deletion of TL1 and RCS2, both located in region II, reduced the amount of sgRNA, the sequence in region II including these two structures seems to be more important, suggesting that some tertiary interactions, particularly pseudoknot interactions, may be also required in the production of nuclease-resistant sgRNA.

It is still unclear why sgRNA is generated in a Dengue-2 virus infection. Corresponding studies in WNV has identified two functions of sgRNA that contribute to viral evasion of the type I

interferon response and display RNA interference suppressor activity (Schnettler et al., 2012; Schuessler et al., 2012). Growing evidence indicates that sgRNA probably plays a role in modulating the host antiviral response via RNA-mediated pathways. Our result suggests that sgRNA may indeed act during virus–host interplay. We have shown that the ability to produce abundant full-length sgRNA is required for virus-induced cytopathicity in cell culture and apoptotic cell death. Interestingly, sgRNA alone without Dengue-2 virus infection did not induce cell death, while it can partially rescue the cytopathicity and also apoptosis of mutant virus defective in sgRNA generation (Fig. 7). It demonstrates that sgRNA must interact with virus in host cells. Therefore we propose that sgRNA might be a viral signaling factor in a DENV-2-induced apoptosis pathway. Additionally, no matter what the origin of sgRNA was, it was always functioning during a Dengue-2 virus infection (Fig. S2). This result suggests that sgRNA may not have species specificity.

To date, cell death caused by flavivirus infection has been associated via several pathways and mechanisms, including necrosis and apoptosis (Ait-Goughoulte et al., 2008; Medigeshi et al., 2007; Ramanathan et al., 2006; Su et al., 2002; Yang et al., 2002). Whether in vitro or in vivo, apoptosis has been implicated as a cytopathologic mechanism in response to Dengue virus infection in various cell types (Courageot et al., 2003). Our findings clarify that the wild type of DENV-2 can induce apoptosis in BHK-21 cells while the mutant virus deficient in sgRNA generation cannot. It is possible the production of sgRNA contributed to the induction of apoptotic cell death after infection. The apoptosis pathway by Dengue-2 virus infection is in a caspase-3 dependent manner, and finally results in the cleavage of PARP.

How does sgRNA lead to apoptotic cell death of Dengue-2 virus infection? Recently accumulated evidence proves that viruses can modulate the PI3K/Akt signaling pathways, and some earlier studies indicates the pathway serves an anti-apoptotic role (Cooray, 2004; Lee et al., 2005). The probability that the PI3k/Akt pathway participates in host cell survival during viral infection has prompted us to investigate the relation between sgRNA and this transduction pathway. Analysis from the Western blotting (Fig. 6) shows that Akt can be phosphorylated after wild type and M8 virus infection; however, the wild type level of Akt phosphorylation decreased at 48 h after infection, while in M8 virus it maintained a constant level, which might then protect cells from apoptosis. Because bcl-2 is one of the major downstream mediators of the PI3k/Akt pathway, the expression of bcl-2 protein was also detected. In wild type and M8 mutant virus the trend of bcl-2 were almost the same as that of the phosphorylated Akt. The protein bcl-2 remained at a high level in M8 virus infected cells, and in wild type it began to reduce at 72 h after infection. Considering the time course, the wild type virus just started apoptosis at 72 h p.i., a later stage of infection (Fig. S1). The accordance between these two proteins rules out that Dengue-2 virus infection initiates at least two pathways: apoptosis transduction to kill the infected cells and survival signaling to hold cells in a status amenable to longer virus progeny production. The sgRNA cells did not sustain the protein levels of phosphorylated Akt at the later time points after virus infection, so the downstream factor bcl-2 subsided and finally the cells underwent apoptosis. Without the sgRNA, cells could hold the level of Akt phosphorylation at a constant level and then up-regulate the bcl-2 protein, and the cells survived. Since sgRNA was also aggregated at the later time points after virus infection, it is indeed of significance in inhibiting PI3K/Akt signaling pathway, and inevitably eliminated the infected cells. In summary, sgRNA is a determinant in Dengue-2 virus-induced apoptosis and is possibly involved in PI3k/Akt signaling pathway through a Bcl-2-related mechanism, resulting in apoptotic cell death.

The data represented here exhibit a novel function of sgRNA in virus-induced apoptotic cell death. Dengue-2 virus has evolved a RNA species to interact with the host cells to balance the apoptotic and antiapoptotic signaling pathway. Whether or not the sgRNA is involved in the interplay between the host cell and the virus decides the outcome of Dengue-2 virus infection. Our study provides useful insight into dengue virus infection and defines a novel function in virus noncoding RNA. Thereafter the experimental result may be applicable to other serotypes of Dengue viruses. Moreover, the virus deficient in production of sgRNA possesses high potentiality for the development of a Dengue-2 virus attenuated vaccine.

Materials and methods

Cells and viruses

Baby hamster kidney (BHK-21) cells and African green monkey kidney (Vero) cells were cultured in Dulbecco's modified Eagle medium (DMEM; Gibco) supplemented with 10% fetal bovine serum (FBS; Gibco) and 1% penicillin/streptomycin in 5% CO_2 at 37 °C. DENV-2 was prepared from a full-length infectious cDNA clone (pACYC TSVFL; strain TSVO1).

Construction of plasmids

Recombinant plasmids were constructed by using an infectious cDNA clone of DENV-2 (pACYC TSVFL; strain TSV01) and a cDNA clone of a *Renilla* luciferase replicon of DENV-2 (pACYC TSV replicon; strain TSV01) (Zou et al., 2011). The mutated DNA fragments were pasted back into the pACYC TSVFL at the *NruI* and *ClaI* sites (nucleotide positions 7735 and 10,921, respectively) and the pACYC TSV replicon at the *XbaI* and *ClaI* sites (nucleotide positions 4908 and 9827, respectively). The primer pairs used for mutagenesis are listed in Table 1. All constructs were verified by DNA sequencing.

RNA preparation and northern blot analysis

Total RNA from the DENV-2-infected cells was extracted with Trizol reagent (Invitrogen) following the manufacturer's instructions. Cytoplasmic/Nuclear RNA was isolated and purified by using Cytoplasmic & Nuclear RNA Purification Kit (Norgen). RNAs were quantified using a NanoDrop spectrophotometer (NanoDrop). About 10 μg of RNA was subjected to denaturing gel electrophoresis in 1.5% agarose and 2% formaldehyde, followed by transfer

Table 1
Primers for mutagenesis[a].

Primer name	Sequence (5′ to 3′)
NS5Mut_F	AGTGCAGCTGCTTGTGTTGTGAAACCCTTAGATG
NS5Mut_R	CATCTAAGGGTTTCACAACACAAGCAGCTGCACT
M1_F	GCAGGAGTCTTGTGGTAGAAGTCAGAAGTCAGGTCG
M1_R	CGACCTGACTTCTGACTTCTACCACAAGACTCCTGC
M2_F	AGGAACATCATGAGACAACCGTCCAAGGACGTTAAA
M2_R	TTTAACGTCCTTGGACGGTTGTCTCATGATGTTCCT
M3_F	GGGAGGCCACAAACCATGCGCATGGCGTAGTGGACT
M3_R	AGTCCACTACGCCATGCGCATGGTTTGTGGCCTCCC
M4_F	TGTACGCATGGCGTAGTGCTCCCTTACAAATCGCAG
M4_R	CTGCGATTTGTAAGGGAGCACTACGCCATGCGTACA
M5_F	GGGGGCCCAAGGTGAGATGTCTCACTGAAAGGACTA
M5_R	TAGTCCTTTCAGTGAGACATCTCACCTTGGGCCCCC
M6_F	CTGTAGTCTCACTGAAAGCCCCGAAATAAAAAACAG
M6_R	CTGTTTTTTATTTCGGGGCTTTCAGTGAGACTACAG
M7_F	AGCCCCGTCCAAGGACGTAAATCTGGGAGGCCACAA
M7_R	TTGTGGCCTCCCAGATTTACGTCCTTGGACGGGGCT
M8_F	CACCTGAGAAGGTGTAAAAACAGCATATTGACGCTG
M8_R	CAGCGTCAATATGCTGTTTTTACACCTTCTCAGGTG

[a] A pair of forward (F) and reverse (R) primers was used to generate mutant replicon and genome length RNAs.

onto Hybond-N membranes (Amersham). Hybridization and visualization were performed using the DIG Northern Starter Kit (Roche).

Primer extension assay

Primer extension analysis was performed as described by Sanbrook et al. (1989). Briefly, total RNA from DENV-2 infected cells was annealed to 5′-biotinylated oligonucleotide which is complementary to DENV-2 nt 10,360 to nt 10,385. Then primer extension reactions were performed using Moloney Murine Leukemia Virus reverse transcriptase (Invitrogen). The products were analyzed in a denaturing 8% polyacrylamide-8M urea sequencing gel. The pACYC TSVFL as a template was run in the same gel to serve as a size and sequence marker.

Transient replicon assay

A transient DENV-2 replicon assay was used to quantify viral translation and RNA replication. BHK-21 cells were electroporated with 10 μg of replicon RNA using a GenePulser Xcell system (Bio-Rad) and an established protocol (Falgout et al., 1993). The transfected cells were re-suspended in 25 ml of DMEM with 10% FBS, seeded into 12-well plates (1 ml/well), and assayed for luciferase activities at the indicated time points.

In vitro transcription, RNA transfection, specific infectivity assay (SIA), and immunofluorescence assay (IFA)

Both genome-length and replicon RNAs of DENV-2 were in vitro transcribed from corresponding cDNA plasmids that were linearized with ClaI. A T7 mMessage mMachine kit (Ambion) was used for RNA synthesis as described previously (Falgout et al., 1993). The RNA transcripts were electroporated into BHK-21 cells and culture fluids were harvested, aliquoted and stored at −80 °C (Zou et al., 2011). For specific infectivity assay (SIA), 1 ml of a series of 1:10 dilutions of the transfected cells were seeded onto confluent BHK-21 cell monolayers (6×10^5 cells per well seeded in a six-well plate 2 days in advance). The seeded cells were allowed to attach to the plates for 5 h before addition of 3 ml DMEM containing 1.2% methyl cellulose (Aquacide II; Calbiochem) and 2% FBS. After 5 days of incubation at 37 °C with 5% CO_2, the cells were fixed in 3.7% formaldehyde (Sigma) and stained with 1% crystal violet. An immunofluorescence assay (IFA) was performed as described previously (Shi et al., 2002), using anti-E monoclonal antibody 4G2 and Texas Red goat anti-mouse IgG as primary and secondary antibodies, respectively.

Plaque assay and growth kinetics

For plaque assays, BHK-21 cells in 12-well plates were infected with a dilution series of viruses. Cells were overlaid with 1.2% methyl cellulose in DMEM containing 2% FBS, incubated at 37 °C for 3 to 4 days, fixed with 3.7% formaldehyde and with 1% crystal violet stained or with immunoperoxidase staining. BHK-21 cells were infected at a multiplicity (MOI) of 1 for 1 h at 37 °C, washed three times with PBS and overlaid with DMEM containing 2% FBS. For growth curves, cell culture fluid from 6-well plates was harvested at the indicated times post infection to determine virus titers by standard plaque assay.

Real-time quantitative PCR analysis

For quantitative PCR, RNA samples were performed with a One Step SYBR PrimeScript Plus RT-PCR Kit (TAKARA). The cycling conditions were as follows: an initial hold at 95 °C for 1 min, followed by 40 cycles consisting of 94 °C for 15 s, and 60 °C for 30 s. The primers used for RT Q-PCR were as follows: ACAGTCTGGAACAGGGTGTGGATT and TTGTTAGCCCAATCAATGAGCCGC. The product was 133 nucleotides in length.

Cytotoxicity assay

Vero and BHK-21 cells were seeded into 96-well plates and infected with MOI=0.1. At 3 to 8 days after infection, CPE was assessed as described previously (Liu et al., 2006). SDH release from cells was measured with MTT Cell Proliferation and Cytotoxicity Assay Kit (Beyotime) according to the manufacturer's instruction.

Complementation analysis

For complementation of a subgenomic RNA deficiency mutant, the fragment of subgenomic nucleotides was inserted into the plasmid pSUPER. Primers for PCR were as follows: CGCGGATCCCCAAGTCAGAAGTCAGGTCGGA and CCCAAGCTTAAAAAAGAACCTGTTGATTCAACAG. To complement sgRNA, BHK-21 cells plated at a density of about 50% were transfected with 500 ng pSUPER-sgRNA and control pSUPER. At 24 h after transfection, cells were infected with the mutant virus.

Apoptosis assay

Apoptosis was assayed by Annexin V-FITC/PI staining following the manufacturer's protocol (Bender MedSystems). Briefly, after 96 h or 120 h of infection, the cells were collected and washed in cold PBS. Then the harvested cells were resuspended in 200 μl 1× binding buffer, Annexin V-FITC (1×) and PI (5 μg/ml) were added to the cells followed by incubation at room temperature in the dark for 10 min. After incubation, 200 μl of 1× binding buffer was added to each sample, and cells were analyzed by flow cytometry (Beckman Coulter EpicsXL).

Antibody and Western blot analysis

Monoclonal antibodies including caspase-3 (#9662), PARP (#9542), bcl-2 (#2876) and phosphor-Akt (Ser473) (#9271) were purchased from Cell Signaling Technology Inc. Monoclonal anti-GAPDH (60004-1-Ig) antibody was purchased from Proteintech Inc. The antiserum of NS1 was stored in our laboratory. For immunoblot analysis, the cells were lysed by cell lysis buffer for Western and IP (Beyotime). Cell lysates were mixed with loading buffer (with β-mercaptoethanol), separated by SDS-PAGE, and transferred to a nitrocellulose membrane (Amersham). The blots were developed with an ECL system (Bio-Rad).

Acknowledgments

The authors are grateful to Pei-Yong Shi (Novartis Institute for Tropical Diseases, Singapore) for technical assistance and valuable comments, Dr. Simon Rayner for critical reading and Gengfu Xiao for providing the pSUPER vector.

This project is supported by Important National Science & Technology Specific Projects (2012ZX10004219, 2012ZX10004403), National Natural Scientific Fund of China (81072675) and Wuhan Key Laboratory on Emerging Infectious Diseases and Biosafety.

Appendix A. Supporting information

Supplementary data associated with this article can be found in the online version at http://dx.doi.org/10.1016/j.virol.2013.09.016.

References

Ait-Goughoulte, M., Kanda, T., Meyer, K., Ryerse, J.S., Ray, R.B., Ray, R., 2008. Hepatitis C virus genotype 1a growth and induction of autophagy. J. Virol. 82, 2241–2249.

Alvarez, D.E., Lodeiro, M.F., Luduena, S.J., Pietrasanta, L.I., Gamarnik, A.V., 2005. Long-range RNA-RNA interactions circularize the dengue virus genome. J. Virol. 79, 6631–6643.

Brinton, M.A., Fernandez, A.V., Dispoto, J.H., 1986. The 3′-nucleotides of flavivirus genomic RNA form a conserved secondary structure. Virology 153, 113–121.

Chu, J.J., Ng, M.L., 2003. The mechanism of cell death during West Nile virus infection is dependent on initial infectious dose. J. Gen. Virol. 84, 3305–3314.

Cooray, S., 2004. The pivotal role of phosphatidylinositol 3-kinase-Akt signal transduction in virus survival. J. Gen. Virol. 85, 1065–1076.

Courageot, M.P., Catteau, A., Despres, P., 2003. Mechanisms of dengue virus-induced cell death. Adv. Virus Res. 60, 157–186.

Despres, P., Flamand, M., Ceccaldi, P.E., Deubel, V., 1996. Human isolates of dengue type 1 virus induce apoptosis in mouse neuroblastoma cells. J. Virol. 70, 4090–4096.

Falgout, B., Miller, R.H., Lai, C.J., 1993. Deletion analysis of dengue virus type 4 nonstructural protein NS2B: identification of a domain required for NS2B-NS3 protease activity. J. Virol. 67, 2034–2042.

Fan, Y.H., Nadar, M., Chen, C.C., Weng, C.C., Lin, Y.T., Chang, R.Y., 2011. Small noncoding RNA modulates Japanese encephalitis virus replication and translation in trans. Virol. J. 8, 492.

Filomatori, C.V., Lodeiro, M.F., Alvarez, D.E., Samsa, M.M., Pietrasanta, L., Gamarnik, A.V., 2006. A 5′ RNA element promotes dengue virus RNA synthesis on a circular genome. Genes Dev. 20, 2238–2249.

Funk, A., Truong, K., Nagasaki, T., Torres, S., Floden, N., Balmori Melian, E., Edmonds, J., Dong, H., Shi, P.Y., Khromykh, A.A., 2010. RNA structures required for production of subgenomic flavivirus RNA. J. Virol. 84, 11407–11417.

Gebhard, L.G., Filomatori, C.V., Gamarnik, A.V., 2011. Functional RNA elements in the dengue virus genome. Viruses 3, 1739–1756.

Gould, E.A., Solomon, T., 2008. Pathogenic flaviviruses. Lancet 371, 500–509.

Gubler, D.J., Kuno, G., Markoff, L., 2007. Flaviviruses. Fields Virology, Fifth ed. Lippincott Williams & Wilkins, Philadelphia, pp. 1153–1252.

Guo, J.T., Hayashi, J., Seeger, C., 2005. West Nile virus inhibits the signal transduction pathway of alpha interferon. J. Virol. 79, 1343–1350.

Hahn, C.S., Hahn, Y.S., Rice, C.M., Lee, E., Dalgarno, L., Strauss, E.G., Strauss, J.H., 1987. Conserved elements in the 3′ untranslated region of flavivirus RNAs and potential cyclization sequences. J. Mol. Biol. 198, 33–41.

Khromykh, A.A., Kenney, M.T., Westaway, E.G., 1998. trans-Complementation of flavivirus RNA polymerase gene NS5 by using Kunjin virus replicon-expressing BHK cells. J. Virol. 72, 7270–7279.

Kummerer, B.M., Rice, C.M., 2002. Mutations in the yellow fever virus nonstructural protein NS2A selectively block production of infectious particles. J. Virol. 76, 4773–4784.

Kyle, J.L., Harris, E., 2008. Global spread and persistence of dengue. Annu. Rev. Microbiol. 62, 71–92.

Lee, C.J., Liao, C.L., Lin, Y.L., 2005. *Flavivirus* activates phosphatidylinositol 3-kinase signaling to block caspase-dependent apoptotic cell death at the early stage of virus infection. J. Virol. 79, 8388–8399.

Lindenbach, B.D., Thiel, H.J., Rice, C.M., 2007. Flaviviridae: the viruses and their replication. Fields Virology. Fifth ed. Philadelphia: Lippincott Williams & Wilkins 1, 1101–1152.

Liu, R., Yue, L., Li, X., Yu, X., Zhao, H., Jiang, Z., Qin, E., Qin, C., 2010. Identification and characterization of small sub-genomic RNAs in dengue 1–4 virus-infected cell cultures and tissues. Biochem. Biophys. Res. Commun. 391, 1099–1103.

Liu, W.J., Chen, H.B., Khromykh, A.A., 2003. Molecular and functional analyses of Kunjin virus infectious cDNA clones demonstrate the essential roles for NS2A in virus assembly and for a nonconservative residue in NS3 in RNA replication. J. Virol. 77, 7804–7813.

Liu, W.J., Wang, X.J., Clark, D.C., Lobigs, M., Hall, R.A., Khromykh, A.A., 2006. A single amino acid substitution in the West Nile virus nonstructural protein NS2A disables its ability to inhibit alpha/beta interferon induction and attenuates virus virulence in mice. J. Virol. 80, 2396–2404.

Markoff, L., 2003. 5′- and 3′-noncoding regions in flavivirus RNA. Adv. Virus Res. 59, 177–228.

Medigeshi, G.R., Lancaster, A.M., Hirsch, A.J., Briese, T., Lipkin, W.I., Defilippis, V., Fruh, K., Mason, P.W., Nikolich-Zugich, J., Nelson, J.A., 2007. West Nile virus infection activates the unfolded protein response, leading to CHOP induction and apoptosis. J. Virol. 81, 10849–10860.

Munoz-Jordan, J.L., G.G. Sanchez-Burgos, M. Laurent-Rolle, A. Garcia-Sastre. 2003. Inhibition of interferon signaling by dengue virus. In: Proceedings of the National Academy of Sciences of the United States of America. 100, pp. 14333–14338.

Pijlman, G.P., Funk, A., Kondratieva, N., Leung, J., Torres, S., van der Aa, L., Liu, W.J., Palmenberg, A.C., Shi, P.Y., Hall, R.A., Khromykh, A.A., 2008. A highly structured, nuclease-resistant, noncoding RNA produced by flaviviruses is required for pathogenicity. Cell Host & Microbe 4, 579–591.

Proutski, V., Gould, E.A., Holmes, E.C., 1997. Secondary structure of the 3′ untranslated region of flaviviruses: similarities and differences. Nucleic Acids Res. 25, 1194–1202.

Ramanathan, M.P., Chambers, J.A., Pankhong, P., Chattergoon, M., Attatippaholkun, W., Dang, K., Shah, N., Weiner, D.B., 2006. Host cell killing by the West Nile Virus NS2B-NS3 proteolytic complex: NS3 alone is sufficient to recruit caspase-8-based apoptotic pathway. Virology 345, 56–72.

Rice, C.M., Lenches, E.M., Eddy, S.R., Shin, S.J., Sheets, R.L., Strauss, J.H., 1985. Nucleotide sequence of yellow fever virus: implications for flavivirus gene expression and evolution. Science 229, 726–733.

Sanbrook, J., Fritsch, E., Maniatis, T., 1989. Molecular Cloning: A Laboratory Manual. Cold Spring Harbor Laboratories. Cold Spring Harbor, NY 6, 179–187.

Schnettler, E., Sterken, M.G., Leung, J.Y., Metz, S.W., Geertsema, C., Goldbach, R.W., Vlak, J.M., Kohl, A., Khromykh, A.A., Pijlman, G.P., 2012. Noncoding flavivirus RNA displays RNA interference suppressor activity in insect and Mammalian cells. J. Virol. 86, 13486–13500.

Schuessler, A., Funk, A., Lazear, H.M., Cooper, D.A., Torres, S., Daffis, S., Jha, B.K., Kumagai, Y., Takeuchi, O., Hertzog, P., Silverman, R., Akira, S., Barton, D.J., Diamond, M.S., Khromykh, A.A., 2012. West Nile virus noncoding subgenomic RNA contributes to viral evasion of the type I interferon-mediated antiviral response. J. Virol. 86, 5708–5718.

Shi, P.Y., Tilgner, M., Lo, M.K., Kent, K.A., Bernard, K.A., 2002. Infectious cDNA clone of the epidemic west nile virus from New York City. J. Virol. 76, 5847–5856.

Silva, P.A., Pereira, C.F., Dalebout, T.J., Spaan, W.J., Bredenbeek, P.J., 2010. An RNA pseudoknot is required for production of yellow fever virus subgenomic RNA by the host nuclease XRN1. J. Virol. 84, 11395–11406.

Su, H.L., Liao, C.L., Lin, Y.L., 2002. Japanese encephalitis virus infection initiates endoplasmic reticulum stress and an unfolded protein response. J. Virol. 76, 4162–4171.

Yang, J.S., Ramanathan, M.P., Muthumani, K., Choo, A.Y., Jin, S.H., Yu, Q.C., Hwang, D. S., Choo, D.K., Lee, M.D., Dang, K., Tang, W., Kim, J.J., Weiner, D.B., 2002. Induction of inflammation by West Nile virus capsid through the caspase-9 apoptotic pathway. Emerg. Infect. Dis. 8, 1379–1384.

Yu, L., Markoff, L., 2005. The topology of bulges in the long stem of the flavivirus 3′ stem-loop is a major determinant of RNA replication competence. J. Virol. 79, 2309–2324.

Yu, L., Nomaguchi, M., Padmanabhan, R., Markoff, L., 2008. Specific requirements for elements of the 5′ and 3′ terminal regions in flavivirus RNA synthesis and viral replication. Virology 374, 170–185.

Zeng, L., Falgout, B., Markoff, L., 1998. Identification of specific nucleotide sequences within the conserved 3′-SL in the dengue type 2 virus genome required for replication. J. Virol. 72, 7510–7522.

Zou, G., Chen, Y.L., Dong, H., Lim, C.C., Yap, L.J., Yau, Y.H., Shochat, S.G., Lescar, J., Shi, P.Y., 2011. Functional analysis of two cavities in flavivirus NS5 polymerase. J. Biol. Chem. 286, 14362–14372.